ELSEVIER

Journal of Organometallic Chemistry 654 (2002) 56–65

Journal of Organometallic Chemistry

www.elsevier.com/locate/jorganchem

Synthesis and redox property of the binuclear Pt(II) complexes bridged by thieno[3,2-*b*]thiophenes

Masaru Sato [a,*], Akiko Asami [a], Genta Maruyama [a], Motoko Kosuge [a], Jyuzo Nakayama [b], Sigekazu Kumakura [b], Takashi Fujihara [b], Kei Unoura [c]

[a] *Chemical Analysis Center, Saitama University, Urawa, Saitama 338-8570, Japan*
[b] *Department of Chemistry, Faculty of Science, Saitama University, Urawa, Saitama 338-8570, Japan*
[c] *Department of Chemistry, Faculty of Science, Yamagata University, Yamagata 990-8560, Japan*

Received 12 September 2001; received in revised form 28 January 2002; accepted 6 March 2002

Abstract

The binuclear Pt(II) complexes bridged by thieno[3,2-*b*]thiophenes were prepared and their redox behavior was measured by cyclic voltammetry. The complexes showed two one-electron quasi-reversible waves and their first redox potentials are comparable with that of ferrocene. The oxidation potentials of the complexes and the related complexes are explained by the result of the MO calculation. The one-electron oxidation of some complexes gave stable oxidized complexes which showed no IT band in the near infrared region. The electronic and EPR spectra suggest that an unpaired electron is localized on the Pt atom. © 2002 Elsevier Science B.V. All rights reserved.

Keywords: Pt(II) complex; Binuclear complex; Thieno[3,2-*b*]thiophene; Thiophenes-bridging; Redox behavior

1. Introduction

The bi- and oligo-nuclear transition metal complexes bridged by an unsaturated organic compound have been vigorously investigated from various viewpoints, i.e. molecular wires, non-linear optics, liquid-phase complexes, and molecular architectures, because electronic communication between the metal centers should lead to unusual physical and chemical properties [1]. Up to this point, many binuclear Pt(II) complexes linked by olefin [2], acetylene [3], benzene [4], and thiophene derivatives [5] were also reported. However, no systematic redox property of these complexes was examined, although some sporadic measurement of cyclic voltammogram was reported [3g,3i]. Much investigation has been carried out in order to propose the fundamental information about electronic communication between the metal centers [6], while few mixed-valence complexes of platinum organometallics were reported except for the coordination compounds, platinum blue and KPC [7]. Recently, the attempt to isolate the Pt(II)/Pt(IV) mixed-valence complex was reported in the biphenyl-bridged binuclear Pt(II) complexes [4d]. It has been clarified, on the other hand, that electron-rich metal sites and electron-rich bridging transporter seem to be advantageous in order to constitute the electron-delocalized system showing a mixed-valence condition [8]. It has been recently reported that thieno[3,2-*b*]thiophene is an excellent electron transmitter between donor and acceptor sites [9]. We now report the synthesis and redox behavior of the binuclear Pt(II) complexes bridged by thieno[3,2-*b*]thiophene and its dimethyl derivative.

2. Results and discussion

2.1. Synthesis and structure assignment

The titled complexes were synthesized using the procedure described by Sonogashira et al. [5a]. 2,5-Dibromothieno[3,2-*b*]thiophene (**1a**) was lithiated with two equivalents of *n*-BuLi in THF and subsequently reacted with Me_3SnCl to give 2,5-bis(trimethylstannyl)thieno[3,2-*b*]thiophene (**2a**) in good yield. Similarly,

* Corresponding author. Fax: +81-48-858-3707.
E-mail address: msato@cacs.saitama-u.ac.jp (M. Sato).

PII: S0022-328X(02)01375-X

2,5-bis(trimethylstannyl)-3,6-dimethylthieno[3,2-*b*]thiophene (**2b**) was obtained. The reaction of **1a** with $(COD)PtCl_2$ in refluxing CH_2Cl_2 afforded the diplatinum(II) complex bridged by thieno[3,2-*b*]thiophene at 2,5-positions, [Cl(COD)Pt(μ-2,5-$C_6H_2S_2$)Pt(COD)Cl] (**3a**), in an excellent yield. The dimethyl analog (**3b**) was prepared from **2b** in a similar manner. Triethylphosphine and tributylphosphine derivatives **4a** and **5a** were produced by ligand exchange of diplatinum(II) complex **3a** with triethylphosphine and tributylphosphine in CH_2Cl_2 at room temperature, respectively. Dimethyl analogs **4b** and **5b** were similarly prepared from **3b** in good yields (Scheme 1). The ^{1}H-NMR spectrum of **4a** showed the methyl signal at δ 1.10 (36H), the methylene protons at δ 1.74 (24H), and the aromatic proton at δ 6.50 (2H), suggesting that COD is exchanged by triethylphosphine. The assignment was also supported by elemental analysis. Similar ^{1}H-NMR spectral evidence was also obtained for **5a**, **4b**, and **5b**. The molecular structure of **5b** was determined by X-ray diffraction. A unit cell contained two crystallographically unique halves of the molecular for **5b**, with the whole molecular located on the inversion center. The two independent molecules had essentially the same structure. The crystallographical data are summarized in Table 1, the ORTEP view of one of the molecules is shown in Fig. 1 and the selected bond distances and bond angles are summarized in Table 2. The Pt–C distances in the independent molecules of **5b** are 2.016(12) and 1.970(16) Å, which are almost the same as those in μ-2,5-thienylene diplatinum complex [1.99(4) and 2.08(3) Å] [5b] and are in the range of the normal Pt–C(sp^2) bond length. The Pt(II) coordination plane in each molecule of **5b** twists to the ring plane of thieno[3,2-*b*]thiophene by 93.37(7) and 92.54(9)° and the dihedral angle between two Pt(II) coordination planes is small (6.7 and 5.0°). These are considerably different from those in the μ-2,5-thienylene diplatinum(II) complex [twist angle: 106.0 and 48.6°; dihedral angle, 48.6°] [5b]. Such differences are probably caused by the presence of the methyl group on the thieno[3,2-*b*]thiophene ring in **5b** and the presence of the bridging propylene chain in the μ-2,5-thienylene diplatinum(II) complex.

Table 1
Crystal and intensity collection data for **5b**

Compound **5b**	
Empirical formula	$C_{56}H_{114}Cl_2P_2S_2Pt_2$
Formula weight	1436.63
Crystal system	Monoclinic
Space group	$P2_1/c$
a (Å)	21.350(2)
b (Å)	13.2660(6)
c (Å)	26.642(3)
β (°)	11.275(4)
V (Å^3)	37031.5(1)
Z	4
D_{calc} (g cm^{-3})	1.357
Crystal size (mm)	0.60 × 0.15 × 0.15
Linear absorption coefficient (cm^{-1})	42.69
Radiation (λ, Å)	Mo Kα (0.71073)
Reflection (hkl) limits	$0 \le h \le 30$, $0 \le k \le 15$, $-37 \le l \le 35$
Total number of reflections measured	17 532
Number of unique reflections	7159
Number of reflections used in L.S.	7159
L.S. parameters	590
R	0.054
R_W	0.059
Maximum peak in final Fourier map (e Å^{-3})	101.01
Minimum peak in final Fourier map (e Å^{-3})	−7.40

2.2. Redox properties

The cyclic voltammograms of the diplatinum(II) complexes (**4a**–**5b**) bridged by thieno[3,2-*b*]thiophene

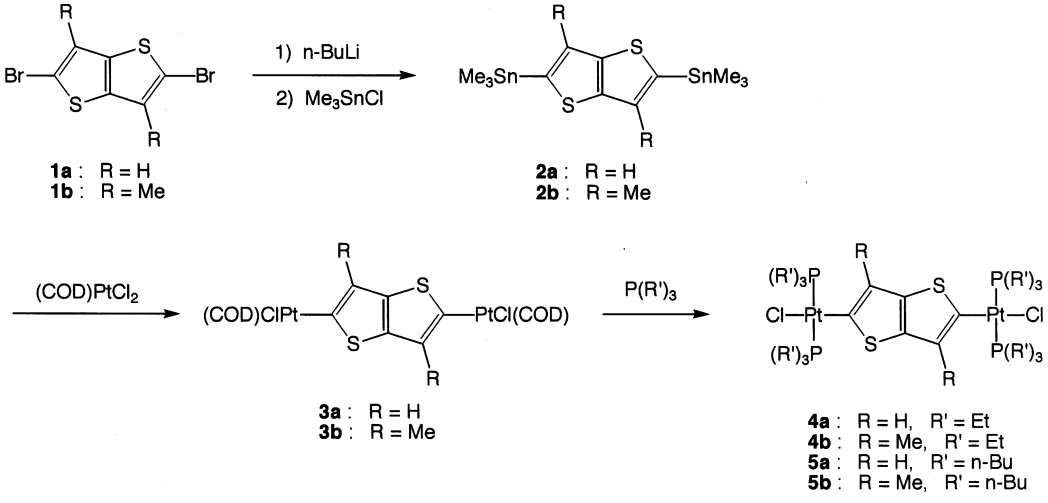

Scheme 1.

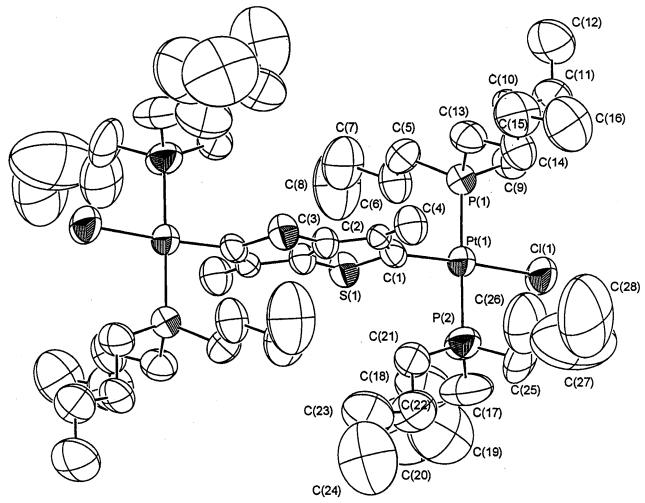

Fig. 1. ORTEP view of one of the molecules of **5b**.

Table 2
Selected bond distances and bond angles for **5b**

Bond distances			
Pt(1)–Cl(1)	2.368(4)	Pt(1)–P(1)	2.296(4)
Pt(1)–P(2)	2.298(5)	Pt(1)–C(1)	2.016(12)
Pt(2)–Cl(2)	2.382(6)	Pt(2)–P(3)	2.278(6)
Pt(2)–P(4)	2.292(6)	Pt(2)–C(31)	1.970(16)
S(1)–C(1)	1.745(12)	S(1)–C(3)	1.719(12)
S(2)–C(31)	1.771(15)	S(2)–C(33)	1.725(15)
C(1)–C(2)	1.434(16)	S(2)–C(3)	1.486(15)
C(31)–C(32)	1.42(3)	C(32)–C(33)	1.43(3)
C(3)–C(3)	1.351(15)	C(33)–C(33)	1.370(17)
Bond angles			
P(1)–Pt(1)–Cl(1)	92.8(2)	P(2)–Pt(1)–Cl(1)	87.8(2)
P(1)–Pt(1)–C(1)	90.1(4)	P(2)–Pt(1)–C(1)	87.3(4)
P(3)–Pt(2)–Cl(2)	88.1(2)	P(4)–Pt(2)–Cl(2)	88.8(2)
P(3)–Pt(2)–C(31)	92.3(5)	P(4)–Pt(2)–C(31)	90.9(5)
S(1)–C(1)–C(2)	114.1(9)	C(1)–C(2)–C(3)	104.8(9)
C(2)–C(3)–C(3)	118.2(10)	S(1)–C(3)–C(3)	110.5(9)
S(2)–C(31)–C(32)	108.9(11)	C(31)–C(32)–C(33)	111.6(13)
C(32)–C(33)–C(33)	115.8(13)	S(2)–C(33)–C(33)	110.0(12)

derivatives at the 2,5-positions were measured in a solution of 0.1 M n-Bu_4NClO_4 in CH_2Cl_2 at a glassy carbon electrode and a sweep rate of 0.1 V s^{-1}. The redox potentials were summarized in Table 3, along with those of the related complexes. For example, complex **4a** showed two redox waves at 0.06 and 0.72 in the scan range between +1.10 V and −1.0 V. In the cyclic voltammogram, the ($E_{pc}-E_{pa}$) values in the first ($i_{pa}/i_{pc}=1.05$) and second waves ($i_{pa}/i_{pc}=1.02$) were 115 and 120 mV, respectively. The thin-layer coulometry of **4a** in CH_2Cl_2 showed $n=1.02\pm0.12$ for the first redox process and the height of the second oxidation peak was very similar to that of the first. These results confirm that either of the two redox waves observed in the cyclic voltammogram of **4a** is due to one-electron redox process. A similar cyclic voltammogram was observed

Table 3
Redox potentials of complexes **4** and **5** and the related complexes (vs. $FcH^{0/+}$)

Complexes	$E_{1/2}$ (1)	$E_{1/2}$ (2)	$\Delta E_{1/2}$
4a	0.06	0.72	0.66
5a	0.07	0.75	0.68
4b	0.01	0.70	0.69
5b	−0.06	0.70	0.82
6	0.03	0.58	0.55
7	0.15	0.98 [a]	
8	0.60	1.18 [a]	

[a] Irreversible wave.

for **4b**, **5a**, and **5b**. In contrast to these compounds, the cyclic voltammograms of the 3,6-dimethylthieno[3,2-*b*]thiophene ($E_{pa}=1.03$ V) and 2,5-bis(trimethylstannyl)-3,6-dimethylthieno[3,2-*b*]thiophene ($E_{pa}=0.84$ and 0.97 V) showed only irreversible oxidation wave.

For the comparison, the cyclic voltammograms of the diplatinum(II) analogs with the μ-2,2′-bithienylene (**6**), μ-2,5-thienylene (**7**), and μ-phenylene bridges (**8**) were measured. The cyclic voltammograms of **5b**, **6**, **7**, and **8** are shown in Fig. 2. Complex **7** with a thienylene bridge exhibited a quasi-reversible wave at 0.15 V and irreversible waves at 0.98 and 1.45 V. The last wave had about double the magnitude of the first and second waves. Complex **8** with phenylene linker showed a quasi-reversible wave at 0.60 V and irreversible waves at 1.18 and 1.42 V. In this case, the i_{pa} value of the second wave was larger than the double i_{pa} value of the first wave and the i_{pa} value wave at 1.42 V is similar to that of the second. These voltammograms suggest that the first and second waves stem from the bridging aromatics and the irreversible wave at high potential is caused by the oxidation of the Pt(II) sites. This suggestion may be supported by the following facts: (i) the acetylene bridged Pt(II) complexes, $Ar(Ar_3P)_2Pt(C{\equiv}C)_nPt(PAr_3)_2Ar$, showed two irreversible oxidation waves ($n=4$, 0.96/1.33 V; $n=6$, 1.19/1.34 V) [10] and the Pt(II) ferrocenylacetylide complexes, $FcC{\equiv}CPt(PPh_3)_2Ar$ (+0.72–+0.95 V) [11], exhibited a two-electron irreversible oxidation. (ii) The redox wave due to the thienylene linker in complex $FcCH{=}CH(C_4H_2S)Pt(PPh_3)_2Br$ was observed at 0.255 V [12]. It is worth noting that the wave in lower potential of **8** is remarkably reversible because of no observation of the wave due to the phenylene linker in $FcCH{=}CH(C_6H_4)Pd(PPh_3)_2I$ [12]. The presence of two Pt(II) metals in the *para*-position of the benzene ring may be responsible with such good reversibility and cathodical shift. Also, there would be a significant stabilizing effect from the Pt(II) sites to stabilize the thienylene and phenylene radical cations resulting from complexes **7** and **8** by one-electron oxidation.

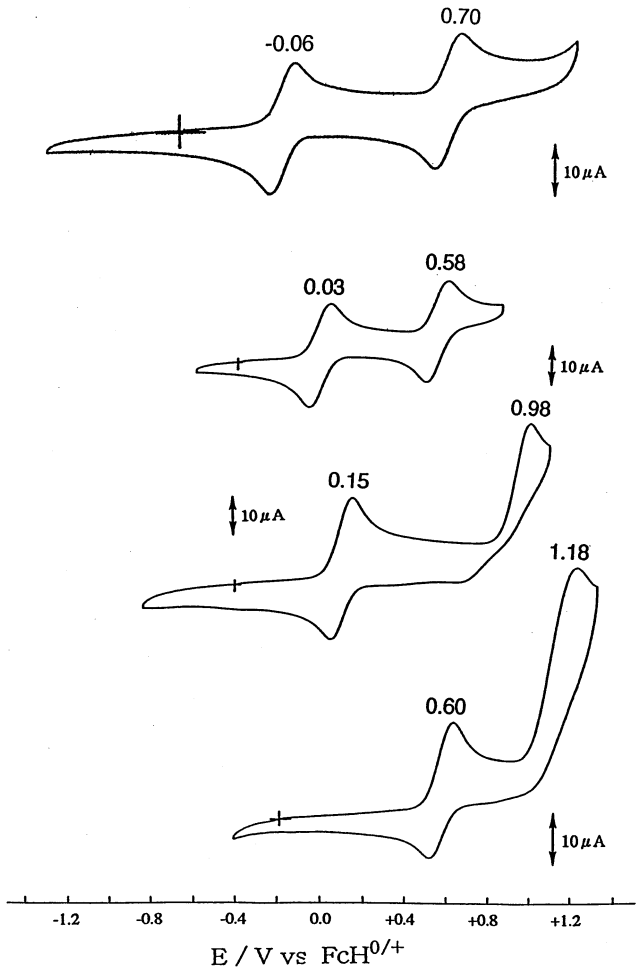

Fig. 2. Cyclic voltammograms of **5b** (upper), **6** (upper middle), **7** (lower middle), and **8** (lower).

Complexes **4**, **5**, and **6**, different from **7** and **8**, showed two quasi-reversible waves in the scan range between + 1.10 V and −1.0 V of their cyclic voltammograms. This redox behavior is also a striking contrast to those of the acetylene bridged Pt(II) complexes, $Ar(Ar_3P)_2Pt(C{\equiv}C)_nPt(PAr_3)_2Ar$, which showed two irreversible oxidation waves [10]. The similar increase of the reversibility of the whole cyclic voltammogram according to the increasing number of the thiophene ring was also reported in the complexes, $H{-}(C_4H_2S)_nRu(dppm)_2Cl$ [13]. It is known that in oligothiophenes, longer oligomers have lower oxidation potentials [14]. Also, a similar shift to the lower potential was observed in the complexes containing oligothiophenes, $Fc[CH{=}CH{-}(C_4H_2S)_n{-}CH{=}CHFc$ [15], $Fc{-}C{\equiv}C{-}(C_4H_2S)_n$ [16], and $H{-}(C_4H_2S)_n{-}Ru(dppm)_2Cl$ [13]. The first oxidation wave in the CV of **6** (0.03 V) is lower than that of **7** (0.15 V) and the difference between the potentials ($\Delta E_p = 0.12$ V) is close to the potential difference ($\Delta E_p = 0.13$ V) observed in complexes, $FcCH{=}CH(C_4H_2S)_nPt(PPh_3)_2Br$ ($n = 1$ or 2) [12]. These facts would suggest that the first and second redox waves of **4**–**6** seem to be due to the loss of an electron from the bridging thiophene derivatives and the low-potential shift of their redox potentials may be related with the increasing conjugation as shown in Scheme 2.

2.3. Theoretical study

For elucidating the electrochemical properties, the electronic features of the preceding complexes **5b**, **6**, **7**, and **8**, were sought computationally. To facilitate the theoretical analysis, the simplified model complexes which the smaller ligand PH_3 was used instead of PPh_3 as the ligand on the Pt(II) atom, $Cl(PH_3)_2Pt{-}Arom{-}Pt(PH_3)_2Cl$ [Arom = C_6H_4 (**8′**), C_4H_2S (**7′**), $C_8H_4S_2$ (**6′**), and $C_8H_8S_2$ (**5b′**)], were adopted. The model compounds were subjected to geometry optimization. Quantitative agreement between the observed and calculated data is not expected due to the nature of the theoretical and structural approximations, but the model complexes can provide an effective method for probing the electronic structures and electrochemical properties of the experimental complexes. The structural parameters obtained from the optimized structure of **5b′** are compared with the crystallographically determined parameters for **5b**. The Pt–C distances [2.032 Å for **5b′** and 2.016 Å for **5b**] are well reproduced, but the S–C [1.833 Å for distances and 1.745 Å for **5b**] and C=C distances [1.362 Å for **5b′** and 1.434 Å for **5b**] are not coincident with each other. In the optimized structure, the electron delocalization in the thieno[3,2-*b*]thiophene ring seems likely to be underestimated.

A simplified representation of the fragment orbital interaction diagram for $[Cl(H_3P)_2Pt]_2^{2+}$ and $[C_8H_8S_2]^{2-}$ of complex **5b′** is presented in Fig. 3. The MO energy levels of **5b′** are shown in the center, the fragment orbital levels for the anionic thieno[3,2-*b*]thiophene bridge are on the right, and the fragment orbital levels for $[Cl(H_3P)_2Pt]^+$ are on the left. The linker ligand orbitals mainly participate in two σ and two π interactions with the $Cl(H_3P)_2Pt$ orbitals. The nonbonding symmetric ($n(a_g)$) and antisymmetric ($n(b_u)$) orbitals, which consist primarily of lone pairs of C-2 and C-5 of thieno[3,2-*b*]thiophene, each interacts with a vacant $[Cl(H_3P)_2Pt]_2$ σ orbital (LUMO) with the appropriate symmetry. (Symmetry labels are from C_{2h} point group.) This interaction forms a strong bonding and antibonding pair, of which only the bonding combination is occupied. The $\pi(a_u)$ and $\pi(a_g)$ orbitals of the $[C_8H_8S_2]^{2-}$ fragment can interact with the d_{xz}-dominant orbital of the $[Cl(H_3P)_2Pt]_2^{2+}$ fragment. This combination newly forms a filled bonding and antibonding MO set which may be considered to be driven from four-electron two orbital interactions. These orbitals form the HOMO and HOMO-2 orbitals of the entire molecule. The HOMO-1 orbital is a nonbonding ligand-based π-orbital. As a result, a simple description of the bonding between the

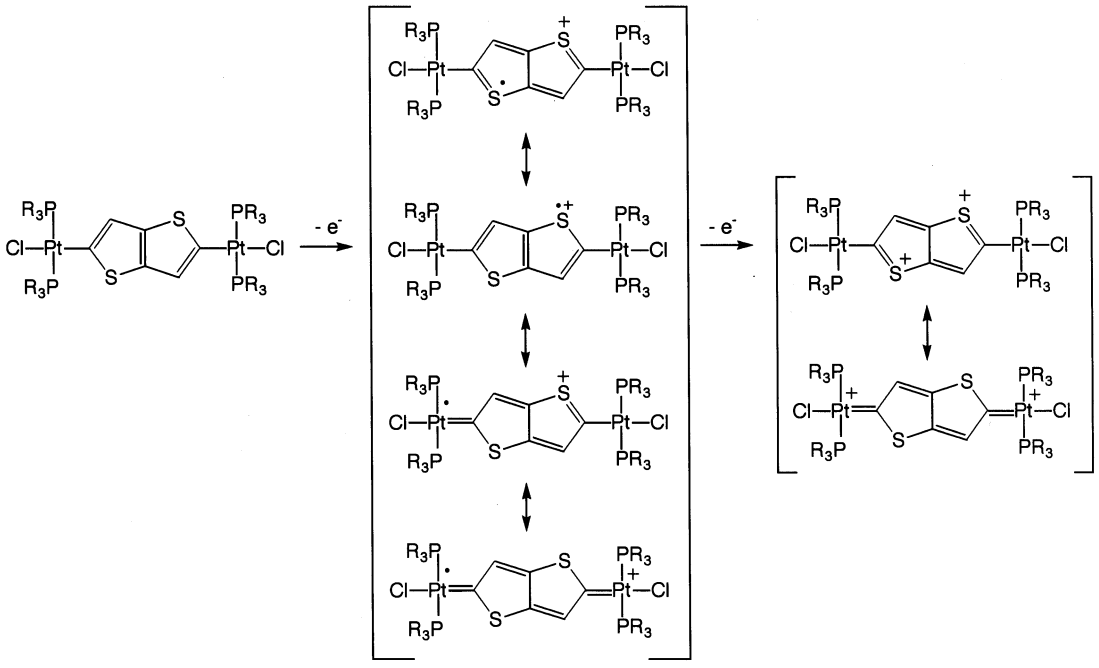

Scheme 2.

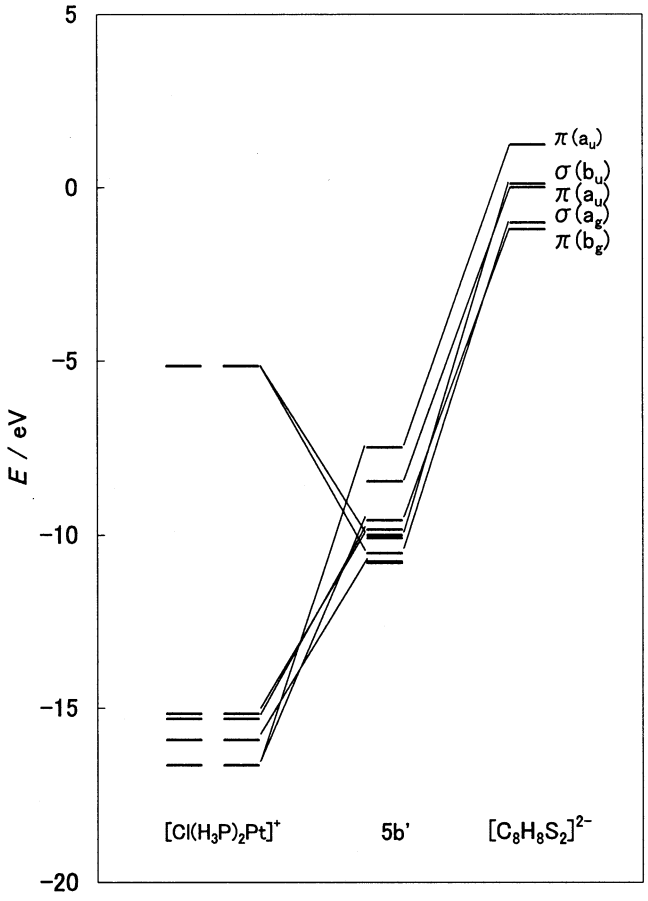

Fig. 3. Schematic MO diagram for model complexes **5b′** depicting the interaction between the frontier orbitals of $[Cl(H_3P)_2Pt]^+$ and $[C_8H_6S_2]^{2-}$.

$[Cl(H_3P)_2Pt]^+$ and $[C_8H_8S_2]^{2-}$ fragments involves a Pt–C single bond and indicates that the metal orbitals do not have a significant net interaction with the π-orbitals of the thiophene ring. The fragment analysis for **7′** also led to a similar result.

Also, the MO calculation of the model complexes **5b′**, **6′**, **7′**, and **8′** showed that the HOMO is a ligand-based orbital, as exemplified in Fig. 4 for **5b′**. This suggests that the loss of an electron from the complexes is largely influenced by the bridging ligand. The energy of the HOMO increases in the following order: **8′** (−0.296) < **7′** (−0.290) < **5b′** (−0.276) < **6′** (−0.267 a.u.). The ascending energy in the complexes probably reflects the lowering HOMO energy of the anionic bridging ligand [**8′** (2.92) > **7′** (2.65) > **5b′** (1.24) > **6′** (0.75 a.u.)], because the HOMO orbital of these complexes is a ligand-based orbital as described above. If electrochemical oxidation involves removal of an electron from the HOMO, the order of the HOMO energy should be in good agreement with that of the redox potentials of complexes [**8** (0.60 V) > **7** (0.15 V) > **6** (0.03 V) > **5b** (−0.06 V)]. The coincidence of both orders is grossly good, but the order for the bithiophene- (**6**) and thienothiophene-bridged complexes (**5**) is reversed. Such reversal cannot be helped, if the theoretical and structural approximation in the calculation and the electrochemical measurement in solvent are considered. Furthermore, it is important to note that the HOMO of complexes **8′**, **7′**, **6′**, and **5b′** is not bonding in nature but consists primarily of an antibonding interaction. This MO picture suggests that there is very little direct

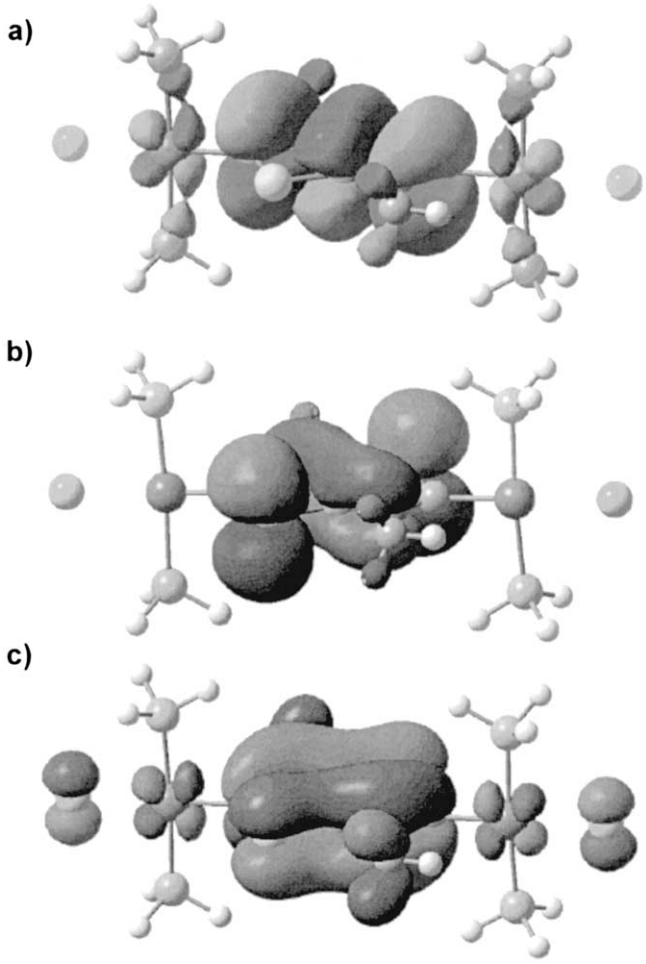

Fig. 4. *iso*-Surface plots (0.02 au) of the HOMO (a), HOMO-1 (b), and HOMO-3 (c) for **5b′**.

communication between the Pt metal sites through the bridging ligand in these complexes.

The MO calculation of the cation radical of **5b′** showed that the HOMO is a ligand-based orbital and the HOMO-1 is a metal-based orbital. The spin density in the cation radical of **5b′** was not located on the Pt metal but almost on the bridging thieno[3,2-*b*]thiophene [0.668 in C(2), −0.258 in C(3), 0.253 in C(3a), −0.147 in S(1), and −0.042 in Pt atoms]. This suggests that the loss of an electron from complex **5b** occurs at the bridging thieno[3,2-*b*]thiophene and the unpaired electron in the oxidized species is almost localized in the linker ligand.

2.4. Chemical oxidation

The result of the cyclic voltammograms suggests that the one-electron oxidized species of **4**, **5**, and **6** is considerably stable, because the first redox wave of them shifts to a low-potential region and is largely separated from the second redox wave. For example, the separation between the first and second redox waves, $[\Delta E_{1/2} = E_{1/2}(2) - E_{1/2}(1)]$, is 0.55 V in **6** and 0.66 V in **4a**. This large separation is comparable with that of the butadiyne bridged diiron, Cp*(dppe)Fe(C≡C)$_2$Fe(dppe)Cp* (0.72 V) [17], and dirhenium complexes, Cp*(NO)(Ph$_3$P)Re(C≡C)$_2$Re(PPh$_3$)(NO)Cp* (0.44 V) [18], which gave a stable one- and two-electron oxidized species. The oxidation of **4a** and **5a** with one equivalent of $AgPF_6$ and DDQ led to the crystalline one-electron oxidized species, **4a**$^{\bullet+}\cdot PF_6$ (**9**) and **4a**$^{\bullet+}\cdot$DDQ$^{\bullet-}$ (**10**), and **5a**$^{\bullet+}\cdot PF_6$ (**11**) and **5a**$^{\bullet+}\cdot$DDQ$^{\bullet-}$ (**12**), respectively (Scheme 3), while a similar oxidation of **4b** and **5b** gave no crystalline one-electron oxidized species, although the oxidation took place. The use of 2.5 equivalents of $AgPF_6$ in the oxidation of **4a** gave only **9** and no two-electron oxidized species, probably because the second oxidizing potential of **4a** is much higher than that of $AgPF_6$. The oxidation of **4a** and **5a** with one equivalent of TCNQ or TCNE afforded only unstable oxidized product. The reduction of the monocation complex **9** with Zn powder in CH_2Cl_2 afforded the corresponding neutral complex, **4a**.

The monocation complexes **9**–**12** are deep-blue or dark-violet plates and stable to air and moisture, with a melting point. The deep-blue solution of **9** in CH_2Cl_2 was very stable since no change in the UV–vis spectrum was observed at all after 1 day at least. The solution gave three vis–UV absorptions at 615.0 (ε 8660), 427.5 (19 500), and 293.5 (6840) nm, while the corresponding neutral complex **4a** showed an absorption band only in a UV region (294.5 nm, ε 20 100), as shown in Fig. 5. Similar vis absorption bands were also observed in **10**–**12**. The absorption band observed in a visible region is probably due to the MLCT or LMCT. No near-IR absorption in **9**–**12** was observed. These results suggest that there is no electronic communication between the Pt metal sites in the oxidized species of diplatinum complexes bridged by thieno[3,2-*b*]thiophene (**9**–**12**). The EPR spectrum of **9** in the solid state at room temperature exhibited an anisotropic signal at $g_{\|}$ 1.995 and $g_{\perp}$ 2.083, although no satellite with ^{195}Pt and no coupling with ^{31}P was observed. This confirms that complex **9** is a radical cation and suggests that the unpaired electron may be localized on the d_z2 orbital of the Pt metal atom, because $g_{\perp} > g_{\|}$. This suggests that the unpaired electron is not delocalized between the two Pt atoms but localized in either of the metal sites. This is not coincident with the result of the MO calculation for the radical cation of **5b′** that the spin density is almost put on the bridging ligand. However, it is possible to consider that the unpaired electron is located on the Pt atom if the theoretical and structural approximations in the calculation are considered, because the MO calculation showed that the HOMO-1 of the radical cation **5b′**$^{+\bullet}$ is a metal-based orbital. Also, the HOMO of complex **5b′** is not bonding in nature but consists primarily of a Pt–C antibonding interaction and so no

4a : R = H
4b : R = Me

9 : R = H, X = PF_6^-
10 : R = H, X = DDQ^-
11 : R = Me, X = PF_6^-
12 : R = Me, X = DDQ^-

Scheme 3.

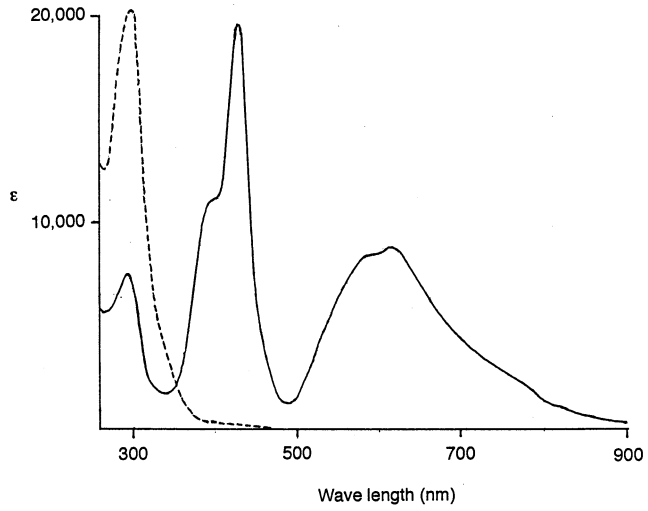

Fig. 5. UV–vis spectra of **4a** (---) and **9** (—) in CH_2Cl_2.

communication between the two metal sites would be expected in the radical cation formed by the loss of an electron from such MO.

In summary, some binuclear platinum complexes bridged by thieno[3,2-*b*]thiophenes were prepared. These complexes showed two quasi-reversible waves of low redox potential in the cyclic voltammogram. The MO calculation of the model complexes indicated that such oxidation waves are due to the loss of an electron from the bridging ligand. In the chemical oxidation with $AgPF_6$ or DDQ, the stable one-electron oxidized species were isolated. Little or no electron delocalization between two metal sites was observed in these one-electron oxidized species.

3. Experimental

All reactions were carried out under an atmosphere of Ar and workups were performed with no precaution to exclude air. NMR spectra were recorded on Bruker AC200, AM400 or ARX400 spectrometers. IR spectra were recorded on Perkin–Elmer System 2000 spectrometer. Cyclic voltammograms were recorded on BAS CV27 or ALS60 in CH_2Cl_2 (freshly distilled from CaH_2 and N_2 purged) solution of 10^{-1} M *n*-Bu_4NClO_4 (polarography grade, Nacalai tesque), and the scan rate was 0.1 V s^{-1}. CV's cells were fitted with glassy carbon (GC) working electrode, Pt wire counter electrode and $Ag \mid Ag^+$ pseudo reference electrode. All potentials were represented vs. $FcH^{0/+}$, which were obtained by the subsequent measurement of ferrocene at the same conditions. Thin-layer coulometry was carried out on the apparatus described earlier [19]. EPR spectrum was recorded on Bruker EMX spectrometer in crystalline state at room temperature.

Solvents were purified by distillation from the drying agent before use as follows: CH_2Cl_2 ($CaCl_2$); diethyl ether ($LiAlH_4$); THF (benzophenone–Na). 2,5-Dibromothieno[3,2-*b*]thiophene [20], 2,5-dibromo-3,6-dimethylthieno[3,2-*b*]thiophene [21], and dichloro(cyclooctadiene)platinum(II) [22], *trans*,*trans*-dichlorotetrakis(tributylphosphine)(1,4-μ-η^1,η^1-phenylene)-diplatinum(II) [23,24], *trans*,*trans*-dichlorotetrakis(tributylphosphine)(2,5-μ-η^1,η^1-thienylene)diplatinum(II) [5a], and *trans*,*trans*-dichlorotetrakis(tributylphosphine)-(2,2′-μ-η^1,η^1-bithienylene)diplatinum(II) [5a], were prepared according to the procedure described in the literature.

3.1. 2,5-Bis(trimethylstannyl)thieno[3,2-b]thiophene (**2a**)

To a solution of 2,5-dibromothieno[3,2-*b*]thiophene (300 mg, 1.0 mmol) in Et_2O (50 ml) was added a 1.5 M solution of *n*-BuLi in hexane (1.6 ml, 2.4 mmol) at 0 °C under Ar. After 10 min, a solution of Me_3SnCl (448 mg, 2.3 mmol) in Et_2O (10 ml) was added to the solution. After stirring at 0 °C for 105 min, the solution was poured into water. The mixture was extracted with Et_2O and the extract was dried over $MgSO_4$. After evaporation under reduced pressure, the residue was dissolved in benzene and the solution was treated with activated carbon. After evaporation, the residue was recrystallized from EtOH to give colorless crystals (295 mg, 66%). M.p. 126–127 °C. Anal. Found: C, 31.08; H, 4.30. Calc. for $C_{12}H_{20}S_2Sn_2$: C, 30.94; H, 4.33%. ^{1}H-NMR ($CDCl_3$, 400 MHz): δ 0.38 (s, $^2J_{SnH} = 28$ Hz, 18H, Me) and 7.25 (s, 2H, =C–H). ^{13}C-NMR ($CDCl_3$, 100 MHz): δ −8.23

(s, $^1J_{SnC} = 176$ and 184 Hz, Me), 126.1 (s, $^1J_{SnC} = 15$Hz, 2-C), 141.2 (3-C), and 147.4 (3a-C).

3.2. 2,5-Bis(trimethylstannyl)-3,6-dimethylthieno[3,2-b]thiophene (**2b**)

This compound was prepared by the similar procedure described in **2a**. Colorless plate, m.p. 154 °C. Anal. Found: C, 34.43; H, 4.82. Calc. for $C_{14}H_{24}S_2Sn_2$: C, 34.05; H, 4.90%. ^{1}H-NMR ($CDCl_3$, 400 MHz): δ 0.40 (s, $^2J_{SnH} = 55$ and 57 Hz, 18H, Me) and 2.35 (s, $^4J_{SnH} = 7$ Hz, 6H, 3C-Me). ^{13}C-NMR ($CDCl_3$, 100 MHz): δ −8.18 (s, $^1J_{SnC} = 350$ and 367 Hz, SnMe), 16.44 (s, $^3J_{SnC} = 15$ Hz, 3C-Me), 134.8 (s, $^1J_{SnC} = 372$ and 386 Hz, 2-C), 136.4 (s, $^2J_{SnC} = 28$ Hz, 3-C), and 147.6 (3a-C). MS (70 eV): *m/z* 493 [M^+].

3.3. 2,5-Bis{chloro(cycloocta-1,5-diene)platinum(II)}thieno-[3,2-b]thiophene (**3a**)

To a solution of **2a** (0.69 g, 1.5 mmol) in CH_2Cl_2 (40 ml) was added dichloro(cycloocta-1,5-diene)platinum(II) (1.1 g, 3.0 mmol). The solution was stirred for 4 h and then the resulting powdery crystals were collected by filtration and washed with CH_2Cl_2. The crystals did not dissolve in common organic solvents. Yellow powdery crystals (1.1 g, 91%), m.p. 229 °C (dec.). Anal. Found: C, 32.13; H, 3.12. Calc. for $C_{22}H_{26}Cl_2Pt_2S_2$: C, 32.40; H, 3.21%.

3.4. 2,5-Bis{chloro(cycloocta-1,5-diene)platinum(II)}-3,6-dimethylthieno[3,2-b]thiophene (**3b**)

This compound was prepared by the similar procedure described in **3a**. Yellow powdery crystals, m.p. 229 °C (dec). Anal. Found: C, 34.36; H, 3.61. Calc. for $C_{24}H_{30}Cl_2Pt_2S_2$: C, 34.17; H, 3.58%.

3.5. trans,trans-Dichlorotetrakis(triethylphosphine)-(2,5-μ-η^1,η^1-thieno[3,2-b]thienylene)diplatinum(II) (**4a**)

To a suspension of **3a** (0.50 g, 0.61 mmol) in CH_2Cl_2 (30 ml) was added triethylphosphine (0.25 g of 10% solution in hexane, 2.1 mmol) under Ar. The mixture was stirred for 4 h. After evaporation, the residue was dissolved in CH_2Cl_2 and the solution was treated with activated carbon and then evaporated. The resulting crystals were recrystallized from CH_2Cl_2 and hexane. Pale yellow crystals (0.49 g, 74%), m.p. 249 °C. Anal. Found: C, 33.95; H, 5.81. Calc. for $C_{30}H_{62}Cl_2P_4Pt_2S_2$: C, 33.62; H, 5.83%. ^{1}H-NMR ($CDCl_3$, 300 MHz): δ 1.10 (p, $J = 8.4$ Hz, 36H, Me), 1.74 (m, 24H, CH_2) and 6.50 (s, 2H, 3,6-H). ^{13}C-NMR ($CDCl_3$, 100 MHz): δ 7.82 (s, Me), 13.18 (t, $^1J_{PC} = 16.6$ Hz, PCH_2), 119.59 (s, $^2J_{PtC} = 66$ Hz, 3-C), 124.48 (t, $^2J_{PC} = 11$ Hz, 2-C), and 143.52 (s, 3a-C).

3.6. trans,trans-Dichlorotetrakis(tributylphosphine)(2,5-μ-η^1,η^1-thieno[3,2-b]thienylene)diplatinum(II) (**5a**)

To a suspension of **3a** (0.10 g, 0.12 mmol) in CH_2Cl_2 (5 ml) was added tributylphosphine (0.11 g, 0.56 mmol) under Ar. The mixture was stirred for 4 h. After evaporation, the residue was chromatographed on activated Al_2O_3 with elution of CH_2Cl_2 and the elute was evaporated. The resulting crystals were recrystallized from EtOH. Pale yellow crystals (76 mg, 44%), m.p. 154 °C. Anal. Found: C, 46.31; H, 7.92. Calc. for $C_{54}H_{110}Cl_2P_4Pt_2S_2$: C, 46.05; H, 7.87%. ^{1}H-NMR ($CDCl_3$, 400 MHz): δ 0.89 (t, $J = 7.2$ Hz, 36H, Me), 1.36 (m, 24H, CH_2), 1.51 (bs, 24H, CH_2), 1.68 (bs, 24H, CH_2), and 6.49 (s, 2H, 3,6-H). ^{13}C-NMR ($CDCl_3$, 100 MHz): δ 13.85 (s, Me), 20.69 (t, $^1J_{PC} = 16.2$ Hz, PCH_2), 20.69 (t, $^2J_{PC} = 6.6$ Hz, PCH_2CH_2), 25.96 (s, $PCH_2CH_2CH_2$), 119.49 (s, $^2J_{PtC} = 66$ Hz, 3-C), 124.76 (t, $^2J_{PC} = 11$ Hz, 2-C), and 143.29 (s, 3a-C).

3.7. trans,trans-Dichlorotetrakis(triethylphosphine)-(2,5-μ-η^1,η^1-3,6-dimethylthieno[3,2-b]thienylene)diplatinum(II) (**4b**)

This complex was prepared similarly from **3b** (0.10 g, 0.12 mmol) according to the procedure described in **4a**. Pale yellow crystals (78 mg, 59%), m.p. 248 °C. Anal. Found: C, 33.39; H, 5.72. Calc. for $C_{32}H_{66}Cl_2P_4Pt_2S_2 \cdot CH_2Cl_2$: C, 33.45; H, 5.78%. ^{1}H-NMR ($CDCl_3$, 400 MHz): δ 1.10 (p, $J = 8$ Hz, 36H, Me), 1.74 (m, 24H, PCH_2) and 2.15 (s, 6H, 3,6-Me). ^{13}C-NMR ($CDCl_3$, 100 MHz): δ 7.97 (s, Me), 13.38 (t, $^1J_{PC} = 16.6$ Hz, PCH_2), 18.67 (s, 3,6-Me), 120.22 (t, $^2J_{PC} = 11$ Hz, 2-C), 125.64 (s, 2-C), and 144.37 (s, 3a-C).

3.8. trans,trans-Dichlorotetrakis(tributylphosphine)-(2,5-μ-η^1,η^1-3,6-dimethylthieno[3,2-b]thienylene)diplatinum(II) (**5b**)

This complex was prepared similarly from **3b** (64 mg, 0.075 mmol) according to the procedure described in **5a**. Pale yellow crystals (45 mg, 42%), m.p. 151 °C. Anal. Found: C, 46.76; H, 8.02. Calc. for $C_{56}H_{114}Cl_2P_4Pt_2S_2$: C, 46.82; H, 8.00%. ^{1}H-NMR ($CDCl_3$, 400 MHz): δ 0.89 (t, $J = 8$ Hz, 36H, Me), 1.34 (m, 24H, CH_2), 1.49 (bs, 24H, CH_2), 1.65 (bs, 24H, CH_2), and 2.15 (s, 2H, 3,6-H). ^{13}C-NMR ($CDCl_3$, 100 MHz): δ 13.78 (s, Me), 18.85 (s, 3,6-Me), 20.99 (t, $^1J_{PC} = 16.2$ Hz, PCH_2), 24.38 (t, $^2J_{PC} = 6.6$ Hz, PCH_2CH_2), 25.97 (s, $PCH_2CH_2CH_2$), 120.60 (t, $^2J_{PC} = 11$ Hz, 2-C), 125.50 (s, 3-C), and 144.13 (s, 3a-C). ^{31}P-NMR ($CDCl_3$, 162 MHz): δ 8.32 ($^1J_{PtP} = 2609$ Hz).

3.9. Oxidation of **4a** with $AgPF_6$

To a solution of $AgPF_6$ (24 mg, 0.094 mmol) in CH_2Cl_2 (10 ml) was added **4a** (0.10 g, 0.094 mmol) under Ar. The solution was stirred for 1 h and then filtered. After being condensed under reduced pressure, the filtrate was diluted with hexane and kept in freezer overnight. The resulting crystals were recrystallized from CH_2Cl_2 and hexane. Deep blue crystals (**9**) (40 mg, 40%), m.p. 149 °C. Anal. Found: C, 29.44; H, 5.04. Calc. for $C_{30}H_{62}Cl_2F_6P_5Pt_2S_2$: C, 29.61; H, 5.14%. UV–vis (CH_2Cl_2): λ_{max} 615.0 (ε 8660), 427.5 (19470), and 293.5 nm (6840). Nir (CH_2Cl_2): λ_{max} 1460 nm (ε 350). IR (nujor mull): 840 cm^{-1} (PF_6).

3.10. Oxidation of **4a** with DDQ

A solution of **4a** (42 mg, 0.039 mmol) and DDQ (8.9 mg, 0.039 mmol) in CH_2Cl_2 was stirred for 4 h under nitrogen. After evaporation, the residual crystals were recrystallized from CH_2Cl_2 and hexane. Dark green crystals (**10**) (15 mg, 26%), m.p. 136 °C (dec.). Anal. Found: C, 36.22; H, 4.11; N, 3.85. Calc. for $C_{46}H_{62}Cl_6N_4O_4P_4Pt_2S_2$: C, 36.21; H, 4.10; N, 3.67%. UV–vis (CH_2Cl_2): λ_{max} 629.5 (ε 2430), 421.0 (7790), and 297.5 nm (15 550). IR (nujor mull): 2231 cm^{-1} (C≡N).

3.11. Oxidation of **4b** with $AgPF_6$

The oxidation was carried out according to the procedure used in the oxidation of **4a**. Dark green crystals (**11**) (61%). UV–vis (CH_2Cl_2): λ_{max} 653.0 (ε 9600), 434.0 (23 500), 396.5 (12 800), and 277.0 nm (6170). IR (nujor mull): 840 cm^{-1} (PF_6).

3.12. Oxidation of **4b** with DDQ

The oxidation was carried out according to the procedure used in the oxidation of **4a**. Dark green crystals (**12**) (61%). UV–vis (CH_2Cl_2): λ_{max} 589.0 (ε 580), 350.5 (11 700), 339.5 (11 100), and 291.5 nm (16 500). IR (nujor mull): 2228 cm^{-1} (C≡N).

3.13. MO calculation

The geometry optimization and orbital calculation of the model complexes, $Cl(PH_3)_2Pt–Arom–Pt(PH_3)_2Cl$ [Arom = C_6H_4 (**8′**), C_4H_2S (**7′**), $C_8H_4S_2$ (**6′**), and $C_8H_8S_2$ (**5b′**)] were carried out using the restricted Hartree–Foch (RHF) method as implemented within the GAUSSIAN 98 software package [25] with a LanL2DZ basis set [26]. Default criteria within the software were employed for geometry optimization. Fragment orbitals were obtained from calculations of the charged fragments $[Cl(H_3p)_2Pt]_2^{2+}$ and $[bridge]^{2-}$, being optimized. Energies of the fragment orbitals were obtained from the corresponding diagonal element of the self-consistent field matrix of the entire molecule. For the case of oxidized species, the structures were fully optimized using the unrestricted open shell formalism and the deviation of the electronic state from a pure doublet was minimal, and Mulliken population analysis was carried out [27].

3.14. Structure determination

The crystallographic data are listed in Table 1 for **5b**. Data collections of crystal data for **5b** were performed at room temperature by the Weissenberg method on Mac Science DIP3000 image processor with graphite monochromated Mo–K_α radiation and an 18-kW rotating anode generator. The structures were solved with the Dirdif–Patty method in Crystan-G (software-package for structure determination) and refined finally by full-matrix least-squares procedure. Absorption correction with the Difab method and anisotropic refinement for non-hydrogen atom were carried out. The hydrogen atoms, located from difference Fourier maps or calculation, were isotopically refined.

4. Supplementary material

Crystallographic data for the structural analysis have been deposited with the Cambridge Crystallographic Data Centre, CCDC no. 170029 for complex **5b**. Copies of this information may be obtained free of charge from The Director, CCDC, 12 Union Road, Cambridge CB2 1EZ, UK (Fax: +44-1223-336-033; e-mail: deposit@ccdc.cam.ac.uk or www: http://www.ccdc.cam.ac.uk).

Acknowledgements

The present work was supported by Grant-in-Aid for Science Research (No. 10640538) from the Ministry of Education, Science and Culture of Japan.

References

[1] (a) W. Beck, B. Niemer, M. Wieser, Angew. Chem. Int. Ed. Engl. 32 (1993) 923;
(b) H. Lang, Angew. Chem. Int. Ed. Engl. 33 (1994) 547;
(c) U.H.F. Bunz, Angew. Chem. Int. Ed. Engl. 35 (1996) 969;
(d) M.D. Ward, Chem. Soc. Rev. (1995) 121;
(e) F. Paul, C. Lapinte, Coord. Chem. Rev. 178–180 (1998) 431;
(f) B. Olenyuk, A. Fechtenkötter, P.J. Stang, J. Chem. Soc. Dalton Trans. (1998) 1707;
(g) R. Ziessel, Synthesis (1999) 1839.
[2] R.J. Puddephatt, M.A. Thomson, Inorg. Chem. 21 (1982) 725.
[3] (a) H. Ogawa, T. Joh, S. Takahasi, K. Sonogasira, J. Chem. Soc. Chem. Commun. (1985) 1220;

(b) H. Ogawa, K. Onitsuka, T. Joh, S. Takahasi, Y. Yamamoto, H. Yamazaki, Organometallics 7 (1988) 2257;
(c) K. Sünkel, U. Birk, C. Robl, Organometallics 13 (1994) 1679;
(d) S. Takahashi, Y. Ohyama, E. Murata, S. Sonogashira, N. Hagihara, J. Polym. Sci. Polym. Chem. Ed. 18 (1980) 349;
(e) R. Nast, J. Moritz, J. Organomet. Chem. (1976) 81;
(f) M.S. Khan, S.J. Davis, A.K. Kakkar, D.J. Schwartz, B. Lin, F.G. Johnson, J. Lewis, J. Organomet. Chem. 424 (1992) 87;
(g) T.B. Peter, J.C. Bohling, A.M. Arif, J.A. Gladysz, Organometallics 18 (1999) 3261;
(h) J. Lewis, N.S. Long, P.R. Raithby, G.P. Shields, W.-Y. Wong, M. Younus, J. Chem. Soc. Dalton Trans. (1997) 4283;
(i) N.J. Long, A.J. Martin, R. Vilar, A.J.P. White, D.J. Williams, M. Younus, Organometallics 18 (1999) 4261.

[4] (a) W.D. Müller, H.A. Brune, Chem. Ber. 119 (1986) 759;
(b) J. Manna, J.A. Whiteford, P.J. Stang, D.C. Muddiman, R.D. Smith, J. Am. Chem. Soc. 118 (1996) 8731;
(c) J. Manna, C.J. Kuehl, J.A. Whiteford, P.J. Stang, Organometallics 16 (1997) 1897;
(d) M.-C. Lagunas, R.A. Gossage, S.L. Spek, G. van Koten, Organometallics 17 (1998) 731.

[5] (a) S. Kotani, K. Shiina, K. Sonogashira, J. Organomet. Chem. 429 (1992) 403;
(b) S. Kotani, T. Adachi, T. Yoshida, K. Onitsuka, K. Sonogashira, Chem. Lett. (1994) 1127.

[6] (a) D.B. Brown (Ed.), Mixed-Valence Compounds, D. Reidel, Boston, MA, 1980.;
(b) D. Astruc, Electron-Transfer and Radical Process in Transition Metal Chemistry (chapter 1), VCH, New York, 1995.

[7] (a) J.S. Miller, A.J. Epstein, Prog. Inorg. Chem. 20 (1976) 1;
(b) J.S. Miller, A.J. Epstein, Ann. N.Y. Acad. Sci. (1978) 313;
(c) J.D. Woollins, P.F. Kelly, Coord. Chem. Rev. 65 (1985) 112.

[8] (a) M. Sato, Y. Hayashi, S. Kumakura, N. Shimizu, M. Katada, S. Kawata, Organometallics 15 (1996) 721;
(b) M. Sato, E. Mogi, M. Katada, Organometallics 14 (1995) 4837.

[9] (a) V.P. Rao, K.Y. Wong, A.K.-J. Jen, K. Drost, J. Chem. Mater. 6 (1994) 2210;
(b) M. Blenkle, P. Bolt, C. Braeuchle, W. Grahn, I. Ledoux, H. Nerenz, S. Stadler, J. Wichern, J. Zyss, J. Chem. Soc. Perkin Trans. 2 (1996) 1337;
(c) O.-K. Kim, A. Fort, M. Barzoukas, M. Blanchard-Desce, J.-M. Lehn, J. Mater. Chem. 9 (1999) 2227.

[10] T.B. Peters, J.C. Bohling, A.M. Arif, J.A. Gladysz, Organometallics 18 (1999) 3261.

[11] M. Sato, E. Mogi, M. Katada, Organometallics 14 (1995) 4837.

[12] K.R.J. Thomas, J.T. Lin, K.-J. Lin, Organometallics 18 (1999) 5285.

[13] Y. Zhu, D.B. Millet, M.O. Wolf, S.J. Rettig, Organometallics 18 (1999) 1930.

[14] F. Martinez, R. Voelkel, D. Naegele, H. Naarmann, Mol. Cryst. Liq. Cryst. 167 (1989) 227.

[15] K.R.J. Thomas, J.T. Lin, Y.S. Wen, Organometallics 19 (2000) 1008.

[16] Y. Zhu, M.O. Wolf, J. Am. Chem. Soc. 122 (2000) 10121.

[17] (a) N. Le Narvor, C. Lapinte, J. Chem. Soc. Chem. Commun. (1993) 357;
(b) N. Le Narvor, L. Toupet, C. Lapinte, J. Am. Chem. Soc. 117 (1995) 7129.

[18] (a) J.W. Seyler, W. Weng, Y. Zhou, J.A. Gladysz, Organometallics 12 (1993) 3802;
(b) M. Brady, W. Weng, Y. Zhou, J. Seyler, A.J. Amoroso, A.M. Arif, M. Böhme, G. Frenking, J.A. Gladysz, J. Am. Chem. Soc. 119 (1997) 775.

[19] K. Unoura, A. Iwase, H. Ogino, J. Electroanal. Chem. Interfacial Electrochem. 295 (1990) 385.

[20] (a) L. Fuller, B. Iddon, K.A. Smith, J. Chem. Soc. Perkin Trans. 1 (1997) 3465;
(b) A. Bugge, Acta Chem. Scand. 23 (1969) 2704.

[21] (a) K.S. Choi, K. Sawada, H. Dong, M. Hoshino, J. Nakayama, Heterocycles 38 (1994) 143;
(b) H. Dong, K. Sawada, A. Ishii, S. Kumakura, J. Nakayama, Tetrahedron 52 (1996) 471.

[22] D. Drew, J.R. Doyle, Inorg. Synth. 13 (1972) 47.

[23] D. Müller, H.A. Brune, Chem. Ber. 119 (1986) 756.

[24] C. Eaborn, K.J. Odell, A. Pidcock, J. Chem. Soc. Dalton Trans. 0 (1978) 357.

[25] M.J. Frisch, G.W. Trucks, H.B. Schlegel, G.E. Scuseria, M.A. Robb, J.R. Cheeseman, V.G. Zakrzewski, J.A. Montgomery, Jr., R.E. Stratmann, J.C. Burant, S. Dapprich, J.M. Millam, A.D. Daniels, K.N. Kudin, M.C. Strain, O. Farkas, J. Tomasi, V. Barone, M. Cossi, R. Cammi, B. Mennucci, C. Pomelli, C. Adamo, S. Clifford, J. Ochterski, G.A. Petersson, P.Y. Ayala, Q. Cui, K. Morokuma, D.K. Malick, A.D. Rabuck, K. Raghavachari, J.B. Foresman, J. Cioslowski, J.V. Ortiz, B.B. Stefanov, G. Liu, A. Liashenko, P. Piskorz, I. Komaromi, R. Gomperts, R.L. Martin, D.J. Fox, T. Keith, M.A. Al-Laham, C.Y. Peng, A. Nanayakkara, C. Gonzalez, M. Challacombe, P.M.W. Gill, B.G. Johnson, W. Chen, M.W. Wong, J.L. Andres, M. Head-Gordon, E.S. Roplogle, J.A. Pople, Gaussian 98, Gaussian Inc., Pittsburgh, PA, 1998.

[26] P.J. Hay, W.R. Wadt, J. Chem. Phys. 82 (1985) 270.

[27] R.S. Mulliken, J. Chem. Phys. 23 (1955) 1833.